

The Effect of Ring Nitrogen Atoms on the Homolytic Reactivity of Phenolic Compounds: Understanding the Radical-Scavenging Ability of 5-Pyrimidinols

Luca Valgimigli,^{*[a]} Giovanni Brigati,^[a] Gian Franco Pedulli,^[a] Gino A. DiLabio,^[c] Marina Mastragostino,^[d] Catia Arbizzani,^[d] and Derek A. Pratt^{*[b]}

Abstract: Six substituted 5-pyrimidinols were synthesized, and the thermochemistry and kinetics of their reactions with free radicals were studied and compared to those of equivalently substituted phenols. To assess their potential as hydrogen-atom donors to free radicals, we measured their O–H bond dissociation enthalpies (BDEs) using the radical equilibration electron paramagnetic resonance technique. This revealed that the O–H BDEs in 5-pyrimidinols are, on average, about 2.5 kcal mol⁻¹ higher than those in equivalently substituted phenols. The results are in good agreement with theoretical predictions, and confirm that substituent effects on the O–H BDE of 5-pyrimidinol are essentially the same as those on the O–H BDE in phenol. The kinetics of the reactions of these compounds with peroxy radicals has been studied by their

inhibition of the AIBN-initiated autoxidation of styrene, and with alkyl and alkoxy radicals by competition kinetics. Despite their larger O–H BDEs, 5-pyrimidinols appear to transfer their phenolic hydrogen-atom to peroxy radicals as quickly as equivalently substituted phenols, while their reactivity toward alkyl radicals far exceeds that of the corresponding phenols. We suggest that this rate enhancement, which is large in the case of alkyl radical reactions, small in the case of peroxy radical reactions, and nonexistent in the case of alkoxy radical reactions, is due to polar effects in the transition states of these atom-transfer reactions. This hypothesis is supported by additional experimental

and theoretical results. Despite this higher reactivity of 5-pyrimidinols towards radicals compared to phenols, electrochemical measurements indicate that they are more stable to one-electron oxidation than equivalently substituted phenols. For example, the 5-pyrimidinol analogues of 2,4,6-trimethylphenol and butylated hydroxytoluene (BHT) were found to have oxidation potentials approximately 400 mV higher than their phenolic counterparts, but reacted roughly one order of magnitude faster with alkyl radicals and at about the same rate with peroxy radicals. The 5-pyrimidinol structure should, therefore, serve as a useful template for the rational design of novel air-stable radical scavengers and chain-breaking antioxidants that are more effective than phenols.

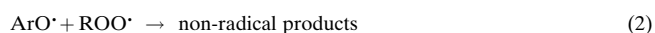
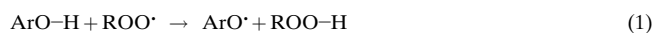
Keywords: antioxidants • lipids • phenols • pyrimidinols • radicals

Introduction

Free-radical chain reactions are of nearly ubiquitous occurrence. Among them, autoxidation and radical polymerization

have attracted the widest attention due to their importance in both natural and industrial processes. As a consequence, chain-breaking radical scavengers, specifically antioxidants and polymerization inhibitors, have become key in the control or prevention of these radical chain reactions. Over the last decade, the role of antioxidants in human health has become even more significant due to the suggested role of free radicals in heart (atherosclerosis), lung (emphysema), and neurodegenerative (Alzheimer's and Parkinson's) diseases, as well as implications in cancer and aging.^[1]

The most important and widely employed chain-breaking radical scavengers for both commercial and therapeutic applications are phenols (ArOH). Their mechanism of action relies on the transfer of their phenolic hydrogen atom to the chain-carrying radical to yield a stable phenoxyl radical that is unable to propagate the chain [Eqs. (1) and (2)]:



[a] Dr. L. Valgimigli, G. Brigati, Prof. G. F. Pedulli
Department of Organic Chemistry "A. Mangini"
University of Bologna, Via S. Donato 15
40127 Bologna (Italy)
Fax: (+39)051-244064
E-mail: valgimig@alma.unibo.it

[b] D. A. Pratt
Department of Chemistry, Vanderbilt University
Nashville, Tennessee (USA) 37235
Fax: (+1)615-343-5478
E-mail: derek.a.pratt@vanderbilt.edu.

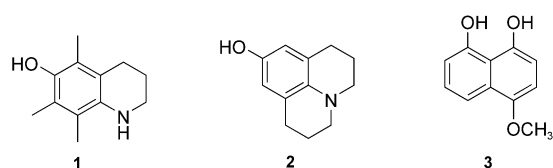
[c] Dr. G. A. DiLabio
National Institute for Nanotechnology
National Research Council, W6-O1O ECERF 9107 116th St.
Edmonton, AB T6G 2V4 (Canada)

[d] Prof. M. Mastragostino, Dr. C. Arbizzani
Istituto di Scienze Chimiche
University of Bologna (Italy)

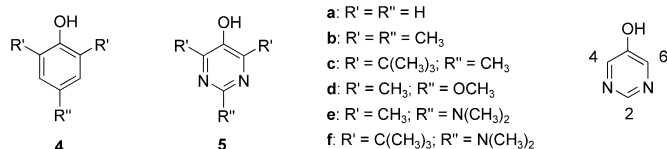
Several investigations have clearly demonstrated that the radical-scavenging ability of phenols is a function of their reactivity toward hydrogen-atom transfer, which in turn depends on their O–H bond dissociation enthalpy (BDE).^[2,3] Electron-donating (ED) groups, especially in the conjugated *ortho*- and *para*- positions relative to the phenolic O–H, weaken the bond and increase the rate of hydrogen-atom transfer to the abstracting radical.^[2] This has so far constituted the major guideline for the rational design of new and more effective phenolic antioxidants.^[4,5] However, there is an important limitation to this approach: while the substitution of phenols with increasingly ED groups (e.g., –NH₂ and –NR₂) decreases the O–H BDEs of phenols it also decreases their ionization (oxidation) potentials (IPs) so that they react directly with oxygen through electron transfer [Eq. (3)], thus reducing their efficacy as antioxidants and giving them pro-oxidant properties:^[4–6]



This is the case, for instance, for an aza analogue of α -TOH (**1**)^[4] and for 9-hydroxyjulolidine (**2**),^[7] which were both found to be relatively useless as antioxidants because of their instability toward air oxidation. Similarly, this was found to be the case for the 1,8-naphthalene diol (**3**),^[8] which was predicted to have a lower O–H BDE than α -TOH by approximately 7 kcal mol⁻¹, but reacted less than twice as fast with peroxy radicals presumably due to decomposition as it yielded dark green solutions that contained a multitude of products upon exposure to air.



We have recently shown that switching from a phenol (**4**) to a pyrimidinol (**5**) structure may be a solution to this problem.^[9] Inspired by our preliminary results we designed a series of substituted 5-pyrimidinols and undertook a systematic study to clarify their interesting homolytic reactivity.

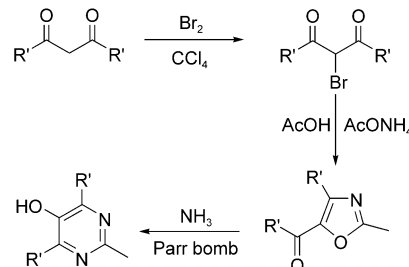


Results

Synthesis of compounds 5a–f: 5-Pyrimidinol (**5a**) was prepared by a modification of the original method proposed by Bredebeck et al.^[10] Briefly, 5-bromopyrimidine was treated with sodium methoxide to yield 5-methoxypyrimidine, which

was subsequently demethylated in good yield by treatment with EtSNa in DMF at 100 °C.

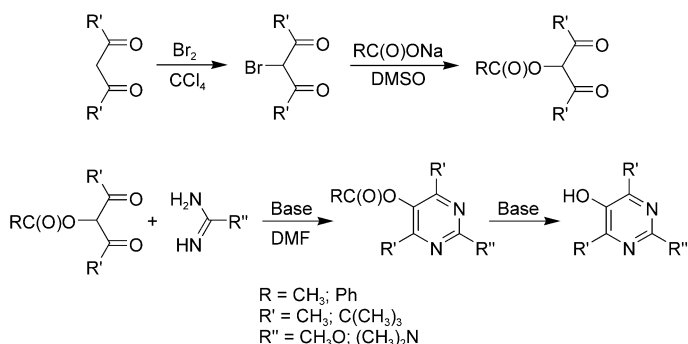
Substituted 5-pyrimidinols bearing an alkyl group in the 2-position (*para* to the phenolic moiety, **5b,c**) were obtained by a procedure developed by Dornow and Hell^[11] and subsequently expanded by Connor and Kostlan as shown in Scheme 1.^[12] Thus, the appropriate α -halodiketone, prepared



Scheme 1.

from the parent diketone as shown, was cyclized to the corresponding 4-acyloxazole by treatment with ammonium acetate in acetic acid. The oxazole was then subjected to ring expansion by reaction with aqueous ammonia in a Parr bomb.

Compounds **5d–f**, bearing a 2-dimethylamino or 2-methoxy group, could be prepared according to the general method of Walker and LaMattina,^[13] by direct condensation of the appropriately substituted guanidine or urea with an α -acyloxydiketone, which is easily accessible from the parent diketone (Scheme 2).



Scheme 2.

While this approach furnished the 2-dimethylamino derivative **5e** in good yield, condensation with the less nucleophilic *O*-methylisourea leading to the 2-methoxy derivative **5d** was much less effective. The di-*tert*-butylated 5-pyrimidinol **5f** was even more problematic due to the steric effects of the terminal *tert*-butyl groups of the 4-acetoxy-2,2,6,6-tetramethyl-3,5-heptadione to attack by the 1,1-dimethylguanidine. Whereas the preparation of **5e** could be accomplished at room temperature, **5f** required heating to 100 °C. Unfortunately, the higher reaction temperature results in some decomposition of the DMF leading to side product formation and some hydrolysis of the acetoxy group leading to some oxidation product formation. Changing the α -acetoxy to benzyloxy and maintaining the reaction temperature around 65 °C in the

condensation step usually provided the most satisfying results. The preparation of **5f** was also achieved by an approach similar to that shown in Scheme 1, by using a 2-aminooxazole in place of the 2-methylloxazole.^[14] All products were stable enough to allow handling in an open atmosphere and could be purified by column chromatography (see the Experimental Section).

EPR spectra of 5-pyrimidinoxyl radicals: In order to confirm our expectation that free radicals would abstract the phenolic hydrogen atom of 5-pyrimidinols to yield 5-pyrimidinoxyl aryloxy radicals, we treated **5a–f** with photolytically generated *tert*-butoxyl radicals, in deoxygenated benzene solutions, inside the cavity of an EPR spectrometer. In the case of **5b–f** this yielded a single paramagnetic species with spectral parameters consistent with the aryloxy radicals derived from abstraction of the phenolic hydrogen atom. A representative spectrum is shown in Figure 1 for the aryloxy radical derived from **5e**. The reaction of *t*BuO• with **5a** leads to very weak EPR signals presumably due to the short lifetime of the corresponding aryloxy radical.

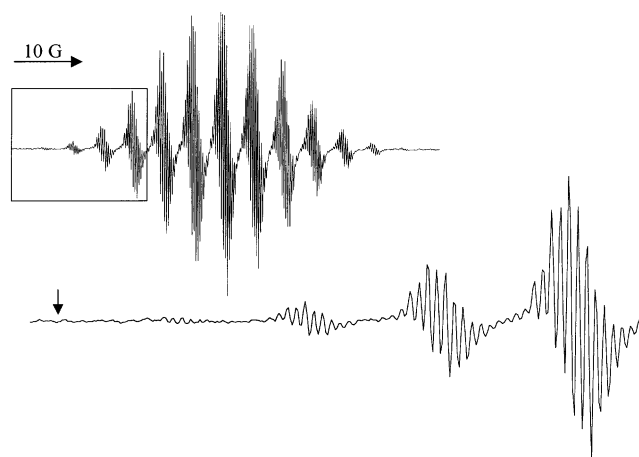
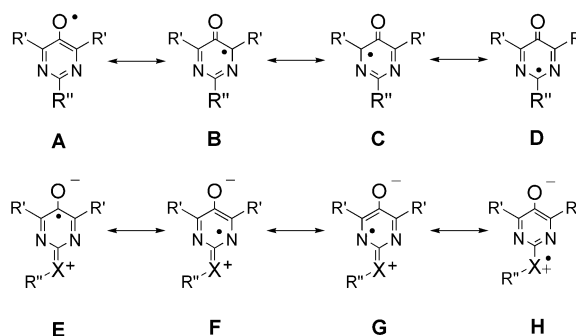


Figure 1. EPR spectrum of 2-*N,N*-dimethylamino-4,6-dimethyl-5-pyrimidinoxyl (derived from **5e**) in benzene at 298 K and its low-field expansion. The arrow indicates the expected position for the center of the first quintet that is not observed due to the low intensity.

The 5-pyrimidinoxyl radicals are characterized by their similar *g* factors ($g = 2.0045 - 2.0047$) and of particular hyperfine patterns (see Table 1), which include small coupling of the pyrimidine ring nitrogens ($a_N = 0.31 - 1.82$ G). The magnitude of these hyperfine splitting constants (Table 1) was found to decrease on increasing the ED character of the substituents in the *ortho*- and *para*-positions relative to the pyrimidinoxyl oxygen. By analogy to the phenoxyl radicals, the 5-pyrimidinoxyl radicals are expected to have an odd alternate spin population pattern with large positive spin densities on the aryloxy oxygen and the 2-, 4-, and 6-positions in the ring, and small negative spin densities on the 5-position and the ring nitrogen atoms (see canonical structures **A–D**, Scheme 3). Upon increasing the ED character of substituents in the 2-position, the higher energy polar structures **E–G**, although normally less important, also contribute to the description of the electronic properties of the 5-pyrimidinoxyl

Table 1. Hyperfine splitting constants and *g* factors of the aryloxy radicals obtained by reactions of 5-pyrimidinols **5b–f** with *tert*-butoxyl radicals in benzene at 298 K.

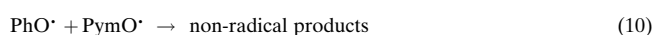
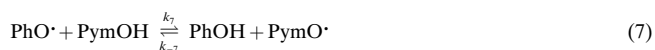
5-Pyrimidinol	$a(N_{1,3})$ [G]	$a(\text{other})/G$	<i>g</i> factor
5b	1.82	6.76 (6H, 2 <i>o</i> -Me)	2.0047
		7.62 (3H, <i>p</i> -Me)	
5c	1.66	0.15 (18H, 2 <i>o</i> -CMe ₃)	2.0047
		9.58 (3H, <i>p</i> -Me)	
5d	1.38	6.54 (6H, 2 <i>o</i> -Me)	2.0045
		1.38 (3H, <i>p</i> -OMe)	
5e	0.31	4.01 (6H, 2 <i>o</i> -Me)	2.0046
		4.81 (1N, <i>p</i> -NMe ₂)	
		4.59 (6H, <i>p</i> -NMe ₂)	
5f	0.32	0.15 (18H, 2 <i>o</i> -CMe ₃)	2.0045
		4.82 (1N, <i>p</i> -NMe ₂)	
		4.73 (6H, <i>p</i> -NMe ₂)	



Scheme 3.

radical. In **E–G**, the spin density pattern is complementary to that predicted for structures **A–D**, that is, positive for the 1-, 3-, and 5-positions and negative for the 2-, 4-, and 6-positions. The decrease of the nitrogen hyperfine splittings observed by increasing the ED character of the substituents in the 2-position can thus be interpreted in terms of an increasing weight of structures **E–G**, inducing opposite spin densities at the 1- and 3-positions with respect to **A–D**.

The O–H bond dissociation enthalpies of 5-pyrimidinols: The O–H bond dissociation enthalpies of **5b–f** were measured using the radical equilibration EPR (REqEPR) technique [Eqs. (4)–(10)].^[15] Thus, when a 5-pyrimidinoxyl radical is generated in the presence of a reference phenol with an O–H BDE close to that of the 5-pyrimidinol under investigation (within ca. ± 2.5 kcal mol⁻¹), an equilibrium is established between the hydrogen-atom-exchanging phenoxyl and 5-pyrimidinoxyl radicals [Eq. (7)].



The EPR spectra recorded under these conditions are actually superpositions of the spectra of the two equilibrating aryloxy radicals from which the molar ratio $[\text{PymO}^\bullet]/[\text{PhO}^\bullet]$ can be obtained and used to determine the equilibrium constant K_7 [Eq. (11)]:

$$K_7 = [\text{PymO}^\bullet][\text{PhOH}]/[\text{PymOH}][\text{PhO}^\bullet] \quad (11)$$

Initial concentrations are chosen such as to avoid significant consumption of the phenol and 5-pyrimidinol during the equilibration experiments (ca. 0.1M).

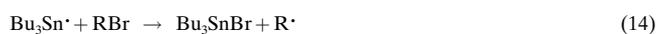
This approach can only be applied if the rate of the hydrogen-atom transfer reaction between the equilibrating species [Eq. (7)] is rapid relative to the decay of the phenoxyl and 5-pyrimidinoxyl radicals [Eqs. (8)–(10)], so that it is the equilibrium concentrations of the two radicals that are actually measured.^[2a] The O–H BDEs can then be calculated from K_7 by means of Equation (12), assuming that the entropy change ΔS^0 for the hydrogen-atom transfer reaction [Eq. (7)] is negligible.

$$\text{BDE}(\text{PymOH}) = \text{BDE}(\text{PhOH}) + \Delta H^0 \cong \text{BDE}(\text{PhOH}) - RT \ln K_7 \quad (12)$$

The validity of this assumption has already been demonstrated with phenols^[2b] and phenothiazines,^[15] and as such we believe it can be safely extended to 5-pyrimidinols. Results are collected in Table 2 together with available O–H BDEs measured previously for equivalently substituted phenols and α -tocopherol. We also include the calculated data from our preliminary communication for comparison.^[9]

Kinetics of reactions with alkyl radicals: The kinetics of the reactions of **5a–f** with alkyl radicals were studied by using the radical clock technique.^[16, 17] This involves the competition between a reference unimolecular process and the bimolecular process under investigation. Here, the 5-*exo* cyclization of the 1-hexenyl radical ($k_r = 2.3 \times 10^5 \text{ s}^{-1}$ at 298 K),^[18] the neophyl radical rearrangement ($k_r = 1.1 \times 10^3 \text{ s}^{-1}$ at 298 K),^[19, 20] and the similar 1,2-aryl migration of 2-methyl-2-(2-naphthyl)-1-propyl (MNP) radical ($k_r = 1.4 \times 10^4 \text{ s}^{-1}$ at 298 K)^[21] were employed to determine the rate constants for hydrogen-atom transfer from 5-pyrimidinols **5a–f** to primary alkyl radicals.

The alkyl radicals were generated in the reaction medium by photolyzing a deoxygenated solution of the corresponding bromide in the presence of hexabutylidistannane, according to the reactions given in Equations (13)–(17):



The alkyl radicals were then allowed to react with the 5-pyrimidinol under investigation, which was present in variable concentration in the reaction mixture. Under conditions chosen to avoid significant consumption of the 5-pyrimidinol during the reaction, the rate constant for hydrogen-atom transfer from the substrate to the primary alkyl radical (k_H) can be obtained by GC (or GC/MS) analysis of the reaction mixture according to Equation (18).^[17, 22]

$$k_H[\text{PymOH}] = k_r \frac{[\text{RH}]}{[\text{R}^{\text{H}}]} \quad (18)$$

All measurements were carried out in benzene except for compounds **5a** and **5b**, due to their limited solubility in this solvent. Therefore, in order to obtain comparable values of k_H along the series of 5-pyrimidinols, the reactivity of **5a** and **5b** in benzene had to be estimated. This was accomplished by taking advantage of the linear free-energy relationship of Equation (19) in which β_S is the Kamlet–Taft–Abraham solvatochromic parameter that describes the hydrogen-bond-accepting ability of a solvent S .^[23, 24] Once the value of the empirical parameter b and that of the rate constant in a non-hydrogen-bonding solvent ($\log k^0$) is determined from experimental values, the value of k^S in benzene ($\beta_S = 0.10$) can be easily obtained by using Equation (19).^[25, 26]

$$\log k^S = \log k^0 + b\beta_S \quad (19)$$

The results are collected in Table 3 together with those for equivalently substituted phenols measured previously^[3] by the same technique.

Table 2. Experimental O–H BDEs in benzene at 298 K for 5-pyrimidinols **5a–f**, phenols **4a–d**, and α -tocopherol.^[a] All values in kcal mol⁻¹.

5-Pyrimidinol	BDE	$\Delta\text{BDE}^{[b]}$	Calcd ^[c] $\Delta\text{BDE}^{[d]}$	Phenol	BDE	ΔBDE^b	Calcd ^[c] $\Delta\text{BDE}^{[d]}$
5a	(90.3) ^[e]	0.0	0.0	4a	88.3 ± 0.8	0.0	0.0
5b	85.20 ± 0.50	– 5.1	– 6.4	4b	82.73 ± 0.18	– 5.6	– 6.7
5c	84.10 ± 0.25	– 6.2	– [f]	4c	81.02 ± 0.13	– 7.3	– [f]
5d	82.48 ± 0.50	– 7.8	– 9.8	4d	80.0 ^[g]	– 8.3	– 10.1
5e	78.16 ± 0.25	– 12.1	– 15.5	4e ^[h]	–	–	– 14.8
5f	76.64 ± 0.10	– 13.7	– [f]	4f ^[h]	–	–	– [f]
				α -TOH	78.23 ± 0.25	– 10.1	– 12.3

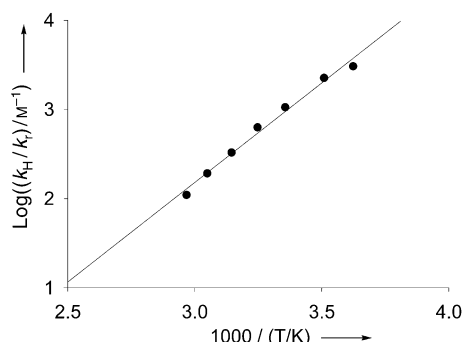
[a] Values for the corresponding phenols (when available) are from reference [2]. Errors correspond to twice standard deviation and do not include the error of the value for the reference phenols used in equilibrations (see Experimental Section). [b] $\Delta\text{BDE} = \text{BDE}(\text{substituted ArOH}) - \text{BDE}(\text{unsubstituted ArOH})$. [c] Using LLM of reference [47]; data from reference [9]. [d] The calculated O–H BDEs in 5-pyrimidinol and phenols are 89.6 and 87.1 kcal mol⁻¹, respectively. [e] This value could not be obtained from EPR equilibrations and was calculated by least-square fitting of the values for compounds **5b,d,e**, **4a,b,d**, and α -TOH to the calculated data (see text). [f] Not calculated. See reference [5]. [g] Calculated from the additive contributions of the substituents; data from reference [2]. [h] Not an air-stable compound.

Table 3. Second-order rate constants for the reactions of 5-pyrimidinols **5a–f**, phenols **4a–c**, and α -tocopherol with primary alkyl radicals at 298 K.^[a]

5-Pyrimidinol	k_H [$M^{-1}s^{-1}$]	Solvent	Phenol	k_H [$M^{-1}s^{-1}$]
5a	$(3.6 \times 10^6)^{[b]}$	PhH	4a	3.4×10^4
	1.64×10^5	CH ₃ CN		
	1.31×10^4	<i>t</i> BuOH		
5b	$(4.6 \times 10^5)^{[b]}$	PhH	4b	8.5×10^4
	5.8×10^4	CH ₃ CN		
	8.6×10^3	EtOAc		
	4.9×10^3	<i>t</i> BuOH		
5c	3.2×10^4	PhH	4c	4.8×10^3
5d	1.4×10^6	PhH		
5e	2.9×10^6	PhH		
5f	7.1×10^5	PhH		
		PhH		

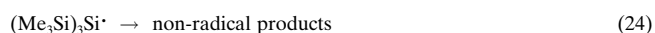
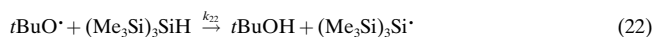
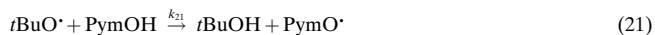
[a] Data for phenols are from reference [3] and were measured by the same technique and under identical experimental conditions. [b] Calculated from linear regression of data measured in the other solvents according to Equation (19) (see text).

The temperature dependence of the rate of hydrogen-atom abstraction by primary alkyl radicals from a representative (vide infra) 5-pyrimidinol (**5d**) was studied by using the neophyl radical rearrangement as the calibrated competing unimolecular process ($\log A = 10.98 \text{ s}^{-1}$, $E_a = 10.83 \text{ kcal mol}^{-1}$)^[19] in the temperature range 237–276 K. The Arrhenius plot is shown in Figure 2, from which the

Figure 2. Arrhenius plot for the reaction of 2-methoxy-4,6-dimethyl-5-pyrimidinol (**5d**) with neophyl radical in benzene.

following parameters can be calculated: $\log A = 6.47 \pm 0.36 \text{ M}^{-1} \text{ s}^{-1}$, $E_a = 0.64 \pm 0.5 \text{ kcal mol}^{-1}$ (value \pm standard error).

Kinetics of reactions with alkoxy radicals: Competition kinetics were also employed to determine the rate constants for hydrogen-atom transfer from **5a–f** to alkoxy radicals. Here, the competition is between two bimolecular processes: the reaction of photolytically generated *t*BuO \cdot with known amounts of 5-pyrimidinol and known amounts of a reference substrate [Eqs. (20)–(24)]. The most appropriate reference substrate was tris(trimethylsilyl)silane (TTMSS), whose rate constant for reaction with *tert*-butoxyl radicals in benzene at 298 K is $k_{19} = 1.0 \times 10^8 \text{ M}^{-1} \text{ s}^{-1}$.^[27]



For some compounds, however, the kinetics have also been investigated by competition with tributyltin hydride ($k^{300\text{K}} = 2.1 \times 10^8 \text{ M}^{-1} \text{ s}^{-1}$)^[28] or Et₃SiH ($k^{300\text{K}} = 5.7 \times 10^6 \text{ M}^{-1} \text{ s}^{-1}$).^[28]

The *tert*-butoxyl radicals were generated by irradiating a solution of di-*tert*-butyl peroxide that contained an internal standard and varying amounts of the silane and one of the 5-pyrimidinols with a high pressure Hg-lamp inside a thermostated (298 K) quartz photoreactor. GC and GC/MS analysis of the reaction mixture before and after UV irradiation provided the desired rate constants from the loss of the starting hydrogen-atom-donating substrate (PyrOH and TTMSS),^[29, 17] according to Equation (25).^[30]

$$\ln \frac{[(\text{Me}_3\text{Si})_3\text{SiH}]_i}{[(\text{Me}_3\text{Si})_3\text{SiH}]_f} = \frac{k_{22}}{k_{21}} \ln \frac{[\text{PymOH}]_i}{[\text{PymOH}]_f} \quad (25)$$

Results are collected in Table 4 together with those available from the literature for some representative phenols, and that for phenol **4b** measured in this work, for comparison.

Table 4. Second-order rate constants for the reactions of 5-pyrimidinols **5a–f**, phenols **4a–b**, and α -tocopherol with *tert*-butoxyl radicals at 298 K.

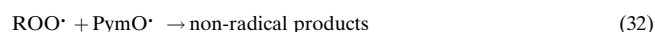
5-Pyrimidinol	k [$M^{-1}s^{-1}$]	Solvent	Phenol	k [$M^{-1}s^{-1}$]
5a ^[a]	$(2.9 \times 10^7)^{[a]}$	PhH	4a ^[b]	2.8×10^8
	1.7×10^7	CH ₃ CN		
	9.5×10^6	<i>t</i> BuOH		
5b ^[a]	$(4.3 \times 10^8)^{[a]}$	PhH	4b ^[c]	8.5×10^8
	3.5×10^8	EtOAc		
	3.3×10^8	<i>t</i> BuOH		
	4.3×10^7	PhH		
5c	4.3×10^7	PhH		
5d	6.7×10^8	PhH		
5e	2.4×10^9	PhH		
5f	5.0×10^8	PhH		
		PhH	α -TOH ^[b]	3.1×10^9

[a] Due to the limited solubility in this solvent, values have been calculated from linear regression of data measured in the other solvents according to Equation (19) (see text) [b] Data from reference [26]. [c] Measured in this work.

Kinetics of reactions with peroxy radicals: The reactions of **5b–f** with peroxy radicals were studied by inhibited autoxidation experiments,^[31] that is, by measuring the inhibition of the AIBN-initiated autoxidation of styrene by the different 5-pyrimidinols in benzene at 50 °C. The rate of oxygen consumption was monitored with an EPR spectrometer by measuring the line-width or the intensity of a spectral line of a persistent nitroxide probe, which was added to the reaction mixture.^[32]

The spin probe employed was tetramethylpiperidine *N*-oxide (TEMPO), which was added to the autoxidizing system in a sufficiently low concentration (usually $5 \times 10^{-6} \text{ M}$) to avoid interference with chain propagation. The three spectral lines of TEMPO ($a_N = 15.52 \text{ G}$, $g = 2.0062$) are initially broadened

by Heisenberg spin exchange with molecular oxygen in the air-saturated benzene solution. As oxygen is consumed by the autoxidation [Eqs. (26)–(30)] the spectral lines become sharper, the line-width being a linear function of the molar oxygen concentration.



When **5d–f** were used as antioxidants, a neat inhibition period of length τ was observed (see Figure 3a). This is due to the competition of reactions in Equations (31) and (32),

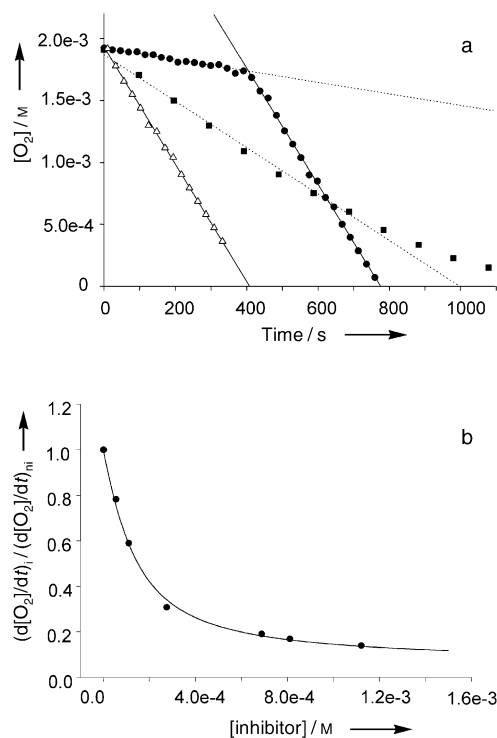


Figure 3. a) Oxygen consumption plot for the autoxidation of 5.19M styrene in benzene containing AIBN (0.0136M) at 323 K, not inhibited (Δ), inhibited by $1.07 \times 10^{-5} M$ **5d** (\bullet), or by $1.07 \times 10^{-4} M$ **5c** (\blacksquare). b) Plot of the ratio of inhibited over not inhibited rate of oxygen consumption versus the concentration of the inhibitor (Darley–Usmar plot) for **5c** at 323 K and numerical fitting of the experimental data according to Equation (36).

representing the chain inhibition by the antioxidant (PymOH), with the chain propagation reaction [Eq. (30)]. At the end of the inhibition period the antioxidant is completely consumed and autoxidation can continue uninhibited. From the length τ the “stoichiometric factor” n , that is, the number

of peroxy radicals trapped by one molecule of antioxidant, could be determined according to Equation (34). The resulting value was $n=2$, similar to α -tocopherol.

$$n = \tau R_i / [\text{PymOH}] \quad (34)$$

The inhibition rate constant k_{inh} , that is, the rate constant for the hydrogen-atom abstraction by peroxy radicals from the 5-pyrimidinol, could instead be obtained from the slope of the inhibition period according to Equation (35), by using α -tocopherol as reference antioxidant^[4] under identical experimental conditions.

$$-\frac{d[O_2]}{dt} = \frac{k_p[\text{styrene}]R_i}{nk_{\text{inh}}[\text{PymOH}]} + R_i \quad (35)$$

The picture was somewhat different with **5b,c** for which a neat inhibition period could not be observed and the oxygen consumption plot showed a unique retarded autoxidation trace (see Figure 3a). This behavior is typical of moderately effective antioxidants that allow chain propagation occur to some extent. In order to obtain the value of k_{inh} for these compounds, a series of inhibited autoxidation experiments were performed under identical experimental conditions ($R_i = 5.0 \times 10^{-8} s^{-1}$; $[\text{styrene}]_0 = 5.19 M$, $T = 323 K$) at different antioxidant concentrations and by plotting the slope of the autoxidation traces versus the antioxidant concentration, according to Equations (36)–(38) developed by Darley–Usmar and co-workers (Figure 3b).^[33]

$$\frac{-(d[O_2]/dt)_i}{-(d[O_2]/dt)_{un}} = 1 - \beta \{ (\alpha[\text{PymOH}] + 1) - (\alpha^2[\text{PymOH}]^2 + 1)^{1/2} \} \quad (36)$$

$$\alpha = \frac{k_{\text{inh}}}{(2k_t R_i)^{1/2}} \quad (37)$$

$$\beta = \frac{k_p[\text{styrene}]}{(2k_t R_i)^{1/2} + k_p[\text{styrene}]} \quad (38)$$

For these 5-pyrimidinols, the value of the stoichiometric factor n could not be determined experimentally, but for calculations it was assumed to be 2 by analogy with the more reactive analogues. No autoxidation inhibiting behavior was observed for the unsubstituted derivative **5a**, whose relatively high (see above) value of BDE make it less reactive toward peroxy radicals than styrene itself, under the experimental conditions employed.

The experimental results are collected in Table 5. Measurements reported by Ingold and co-workers for phenols **4b** and **4c**,^[4] were repeated under experimental conditions identical to those employed for the 5-pyrimidinols for direct compar-

Table 5. Second-order rate constants for the reactions of 5-pyrimidinols **5b–f**, phenols **4b,c**, and α -tocopherol with peroxy radicals in benzene at 323 K.

5-Pyrimidinol	$k_{\text{inh}} [M^{-1}s^{-1}]$	Phenol	$k_{\text{inh}} [M^{-1}s^{-1}]$
5b	3.3×10^4	4b	1.1×10^5
5c	2.2×10^4	4c	1.8×10^4
5d	2.1×10^5		
5e	8.6×10^6		
5f	4.6×10^6	α -TOH	$4.1 \times 10^{6[a]}$

[a] Reference value obtained from reference [4] as described in reference [15].

ison.^[9] Results were essentially indistinguishable from the original values.

Calculated barrier heights for hydrogen-atom abstraction from 5-pyrimidinols by alkyl and peroxy radicals: To complement the kinetic data, we computed the structures and energetics of the transition states for hydrogen-atom abstraction from both 5-pyrimidinol and phenol by the methyl and hydroperoxyl radicals. We used the B3LYP/6–31 + G(d,p) level of theory to perform geometry optimizations on the reactants, transition structures, and products, as well as the hydrogen-bonded pre- and post-reaction complexes that lie along the reaction coordinates for reactions that involve the hydroperoxyl radicals. We also computed single-point energies using a larger basis set (6–311 + G(2d,2p)). For comparison, we performed additional single-point energy calculations using the MPW1K/6–31 + G(d,p) method of Lynch et al.^[34] This approach has been shown to predict hydrogen-atom transfer reaction barrier heights with a mean unsigned error of 1.5 kcal mol⁻¹.^[35] The results are shown in Table 6.

Table 6. Calculated^[a] activation energies and reaction enthalpies for hydrogen atom abstraction from phenol and 5-pyrimidinol by methyl and hydroperoxyl radicals. Energies relative to reactants. All values in kcal mol⁻¹.

	ArO = C ₆ H ₅ O			ArO = C ₄ H ₃ N ₂ O		
	I	II	III	I	II	III
	ArO–H + ·CH ₃ → ArO· + H–CH ₃					
<i>E_a</i>	6.2	7.5	10.2	5.8	7.0	9.5
ΔH	-21.9	-20.6	-19.0	-19.0	-18.1	-16.6
	ArO–H + ·OOH → ArO· + H–OOH					
ArO–H...·OOH ^[b]	-4.4	-4.0	-4.5	-5.6	-5.1	-5.6
[ArO...H...·OOH] [†]	+3.4	+5.1	+14.7	+5.3	+6.6	+15.1
ArO...H–OOH ^[c]	-8.1	-7.0	-5.6	-3.6	-3.0	-1.7
<i>E_a</i> ^[d]	+7.8	+9.1	+19.2	+10.9	+11.7	+20.7
ΔH	+0.6	+1.0	+3.2	+3.5	+3.6	+5.6

[a] I = B3LYP/6–31 + G(d,p)//B3LYP/6–31 + G(d,p) II = B3LYP/6–311 + G(2d,2p)//B3LYP/6–31 + G(d,p) III = MPW1 K/6–31 + G(d,p)//B3LYP/6–31 + G(d,p). [b] Hydrogen-bonded pre-reaction complex. [c] Hydrogen-bonded post-reaction complex. [d] Activation energy is the difference in energy between the hydrogen-bonded pre-reaction complex and the transition structure.

Oxidation potentials of 5-pyrimidinols: To better understand the propensity of the 5-pyrimidinols to undergo one-electron oxidation we have measured the oxidation potentials of **5a–f** by cyclic voltammetry. For comparison, the same measurements were made under the same conditions on the equivalently substituted phenols **4a–c** and α -tocopherol. The measurements were made with a Pt working electrode and Ag/Ag⁺ reference electrode in acetonitrile containing 0.5 M Et₄NBF₄ as electrolyte at a scan-rate of 100 mV s⁻¹.

Reversible redox cycles were obtained only with 5-pyrimidinol **5e**, from which the standard potential was calculated, $V^\circ = +0.55$ V versus SCE. Non-reversible voltammograms were obtained for 5-pyrimidinols **5b–d,f**, phenols **4a–c** and α -tocopherol investigated for scan rates up to 200 mV s⁻¹ at 298 K. This is consistent with previously reported electrochemical behavior of phenols^[36] and is expected given the

increased electron deficiency of radical cations derived from the electron-poor 5-pyrimidinol ring. No neat oxidation peak was observed for the unsubstituted 5-pyrimidinol (**5a**) up to 1.6 V versus Ag/Ag⁺ (1.9 V vs SCE); after this value the background current from the electrolyte oxidation prevented the observation of the supposedly weak signal for the oxidation of the poorly soluble compound **5a**. The electrochemical behavior was found to be independent of the working electrode employed (platinum or glassy carbon), but the renewal of the working-electrode surface, as well as the exclusive use of freshly prepared solutions of the compounds, appeared to be a key feature in order to obtain reproducible results. Results, referred to the SCE electrode, are collected in Table 7.

In order to evaluate whether the oxidation potentials correlate with the HOMO–LUMO energy gaps (vide infra), UV-visible spectra of 5-pyrimidinols **5a–f**, phenols **4a–c**, and α -tocopherol were measured in the same solvent (CH₃CN) and the maximum absorption wavelengths are reported alongside the corresponding E_{ox} in Table 7.

Table 7. Experimental oxidation peak potentials in 0.5 M Et₄NBF₄ in acetonitrile and UV-visible spectral parameters recorded in acetonitrile for 5-pyrimidinols **5a–f**, phenols **4a–c** and α -tocopherol at 298 K.

Compound	E_{ox} vs SCE [V]	λ_{max} [nm]	ϵ_{molar} [L mol ⁻¹ cm ⁻¹]
4a	1.83	272	925
5a	(2.68) ^[a]	270	2011
4b	1.45	280	743
5b	1.82	270	4214
4c	1.34	279	1492
5c	1.80	267	4950
5d	1.33	290	5604
5e	0.55	327	4007
5f	0.75	321	3808
α -TOH	0.89	295	3374

[a] Only a lower limit for this value could be obtained directly from cyclic voltammetry (1.9 V); this value was calculated by least-square fitting of the values for compounds **5b–f** to the calculated data (see text).

Discussion

DFT calculations predict that the presence of two nitrogen atoms in the phenolic ring at the 3- and 5-positions relative to the phenolic hydroxyl produces a moderate increase in the O–H BDE of 2.5 kcal mol⁻¹ (89.6 versus 87.1 kcal mol⁻¹, respectively).^[9] This is best understood as being the result of both a stabilization of the aromatic π system by the more electronegative nuclei in the parent aryl alcohol and the destabilization of the electron-poor aromatic π system in the aryloxy radical. At the same time, this is expected to increase the ionization (oxidation) potential of these compounds substantially (about 24 kcal mol⁻¹ by DFT^[9]), since now the effect of the electronegative atoms in the radical cation will be far more destabilizing than on the uncharged radical. These ideas are illustrated in Figure 4.

Unfortunately, we were unable to obtain both the O–H BDE and oxidation potential in the unsubstituted 5-pyrimi-

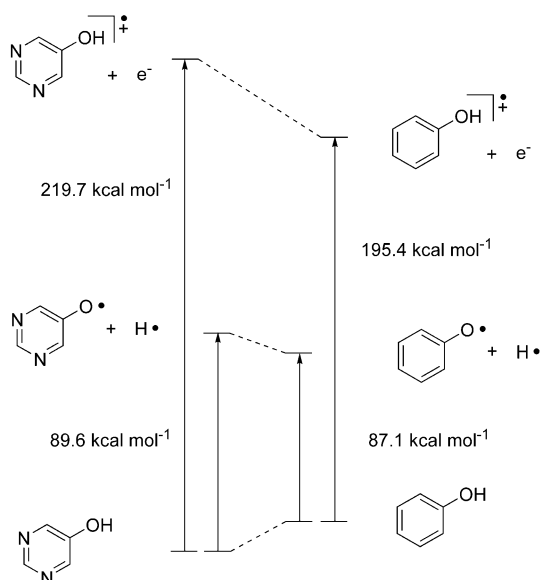


Figure 4. Schematic representation of the effects of incorporating nitrogen in the aromatic ring on the relative stabilities of phenol, phenoxyl, and the phenoxyl radical cation as predicted by DFT calculations.

dinol (**5a**) to directly compare with the values measured for the unsubstituted phenol (**4a**). However, the fact that we cannot measure these values for 5-pyrimidinol, but we can for phenol, indicates that both the O–H BDE and oxidation potential for **5a** are indeed greater than for phenol. We are, nevertheless, able to make estimates of what these values would be under the current experimental conditions by using correlations between the other experimental data and our calculated data. A correlation of the calculated and experimental O–H BDEs in phenols and 5-pyrimidinols is presented in Figure 5. Clearly, there is an excellent correlation between them. Thus, an “experimental” solution-phase (benzene) value for the O–H BDE in the unsubstituted 5-pyr

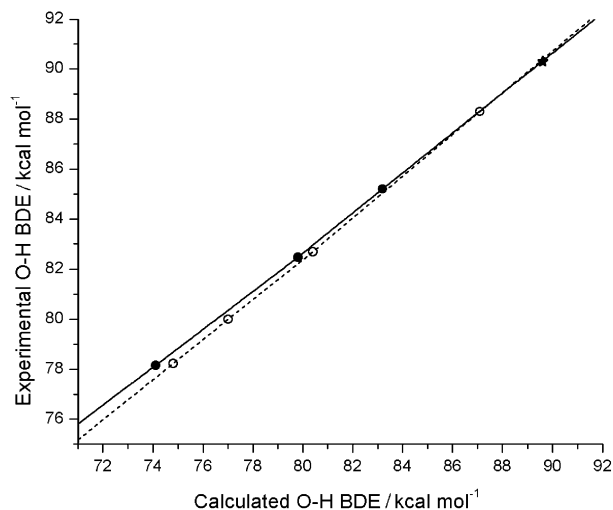


Figure 5. Correlation of the radical equilibration-derived experimental O–H BDEs in benzene at 298 K with the DFT-calculated gas-phase O–H BDEs at 298 K in 5-pyrimidinols (●, solid line) and phenols (○, dashed line). The star indicates the derived solution-phase BDE for the unsubstituted 5-pyrimidinol **5a**.

imidinol can be derived from its calculated value of $89.6 \text{ kcal mol}^{-1}$. This value, $90.3 \text{ kcal mol}^{-1}$, is $2.0 \text{ kcal mol}^{-1}$ greater than that in phenol ($88.3 \text{ kcal mol}^{-1}$)^[2] in good agreement with the predicted gas-phase difference of $2.5 \text{ kcal mol}^{-1}$. This point is represented with a star in Figure 5.

In Figure 6a a similar correlation of the calculated adiabatic gas phase IPs in phenols and 5-pyrimidinols and their corresponding experimental oxidation potentials is presented.

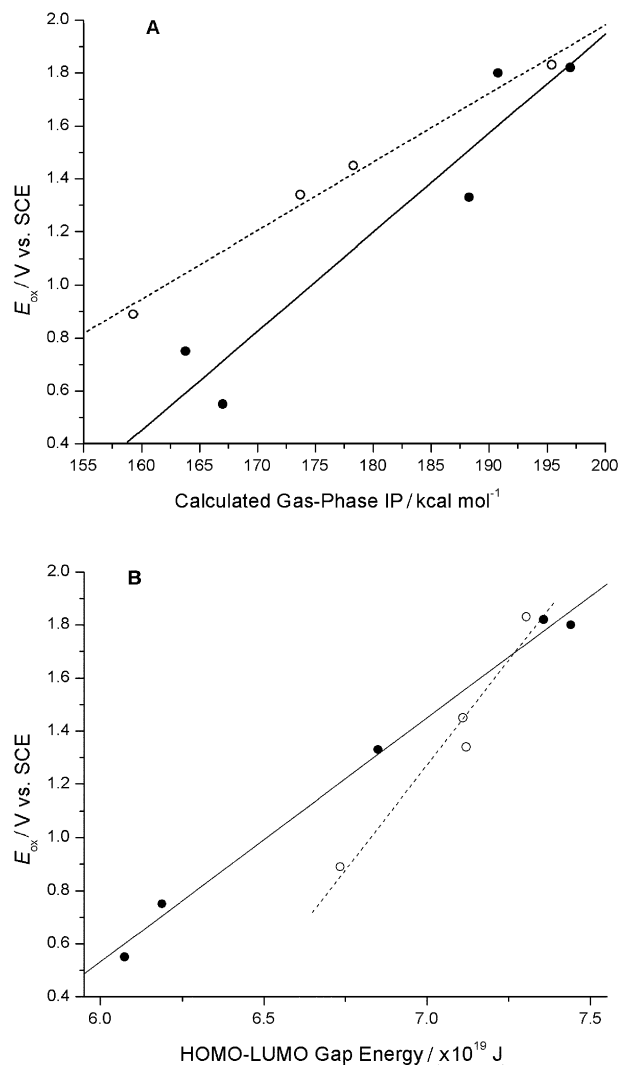


Figure 6. Correlations of the experimental oxidation potentials versus A) the calculated gas-phase adiabatic ionization potentials (0 K) and B) the HOMO–LUMO gap energy as determined by UV-visible absorption spectroscopy in 5-pyrimidinols (●, solid lines) and phenols (○, dashed lines).

Here, the correlation is only satisfactory. Not surprisingly, solvent effects change things considerably and also differently for phenols and 5-pyrimidinols (vide infra). Again, we can derive an “experimental” solution-phase (acetonitrile) value for the oxidation potential of the unsubstituted 5-pyrimidinol from the calculated IP of $219.7 \text{ kcal mol}^{-1}$.^[9] This value, $2.6(8) \text{ V}$, is 850 mV greater than that in phenol (1.83 V), corresponding to approximately $19.6 \text{ kcal mol}^{-1}$ in free en-

ergy, in reasonable agreement with the increase in the calculated gas-phase IP of 24.3 kcal mol⁻¹.

Interestingly, both the substituent effects on the O–H BDEs and the IPs in 5-pyrimidinols were predicted by theory to be largely preserved compared to phenols, as was clearly shown by roughly parallel Hammett-type plots of computed O–H BDEs and IPs versus σ_p^+ for substituents *para* to the O–H moiety for mono-substituted phenols and 5-pyrimidinols.^[9] This theoretical prediction is nicely borne-out by the substituent effects measured by EPR and presented in Table 2.

The situation is not as simple for the experimental oxidation potentials. As can be seen from Table 6, 5-pyrimidinols are very stable toward one-electron oxidation, and their oxidation potentials are significantly higher than that of phenols bearing the same set of substituents (e.g., ca. +400 mV for **5b–4b** and **5c–4c**). This fully confirms our predictions based on calculated (DFT) ionization potentials (IPs).^[9] As we have already pointed out, when the calculated adiabatic IPs are plotted against the experimental E_{ox} values, good linear correlations (Figure 6a) are obtained both for phenols ($R^2 = 0.989$) and 5-pyrimidinols ($R^2 = 0.911$). However, unlike for the similar plot of gas-phase calculated O–H BDEs and experimental BDEs determined in benzene (Figure 5), the two families of compounds do not fall on a single regression line in Figure 6. This can be explained by more substantial solvent (acetonitrile) effects on the heterocyclic substrate and, more importantly, on the corresponding radical cation with respect to the phenolic redox couple. Conceivably, the stronger solvent interactions with the 5-pyrimidinol radical cations as compared to the phenol radical cations give way to lower oxidation potentials. Interestingly, on going from the 4,6-dimethylated to the 4,6-di-*tert*-butylated compounds, the E_{ox} increases (0.75 V for **5f** versus 0.55 V for **5e**) or does not really change (1.82 V for **5b** versus 1.80 V for **5c**) for the 5-pyrimidinols we studied. This is opposite to the trend for phenols (e.g., 1.45 V for **4b** versus 1.34 V for **4c**), and opposite to the calculated gas-phase IPs for both the phenols and 5-pyrimidinols, suggesting that perhaps in the 4,6-di-*tert*-butylated 5-pyrimidinols, the preferential solvation is slightly attenuated. The reliability of the electrochemical measurements is nicely corroborated by correlations of the oxidation potentials with the HOMO–LUMO electronic transition energy both with 5-pyrimidinols ($R^2 = 0.993$) and phenols ($R^2 = 0.950$) (see Figure 6b).

With the role of the ring nitrogen atoms on the hydrogen-atom transfer and electron-transfer thermochemistry of 5-pyrimidinols now relatively well characterized both theoretically and experimentally, we turn to their effects on the kinetics of reactions of these compounds with free radicals. It has been shown elsewhere that within the same series of antioxidants a good linear free-energy relationship exists between the BDE of the bond being broken upon attack from the radical species and the logarithm of the bimolecular rate constant for the reaction with that radical.^[2, 3, 15] An examination of Tables 2–5 reveals that, at least to a qualitative level, the same holds true for 5-pyrimidinols, that is, the relative reactivity of 5-pyrimidinols toward alkyl, alkoxy, and peroxy radicals depends on the magnitude of the O–H BDE,

once the contribution from steric hindrance has been taken into account.^[37] However, a closer look at the data in these tables allows an unexpected observation to be made: while the reactivity of 5-pyrimidinols toward alkoxy radicals (Table 4) is roughly indistinguishable to that of phenols of the same or comparable O–H BDE, the reactivity of 5-pyrimidinols toward peroxy radicals (Table 5) is very close to that of phenols with the same set of substituents despite the larger O–H BDE (ca. 2.5 kcal mol⁻¹). Indeed the values of k_{inh} are 3.3×10^4 and 1.1×10^5 M⁻¹ s⁻¹ for **5b** and **4b**, respectively, with a ratio $k_{inh(5b)}/k_{inh(4b)} \sim 0.3$, and 2.2×10^4 and 1.8×10^4 M⁻¹ s⁻¹ for **5c** and **4c**, respectively, with a ratio $k_{inh(5c)}/k_{inh(4c)} \sim 1$. Furthermore, despite the fact that **5e** has essentially the same O–H BDE and the same steric crowding around the reaction center of α -tocopherol (the reference phenolic antioxidant), it is more than twice as reactive than α -tocopherol itself, and thus is among the most effective antioxidants known ($k_{inh} = 8.6 \times 10^6$ M⁻¹ s⁻¹ at 323 K).

Even more significant is the high reactivity displayed by 5-pyrimidinols toward alkyl radicals (Table 3) relative to phenols with the same set of substituents, for example, **5c** ($k_H = 3.2 \times 10^4$ M⁻¹ s⁻¹) and **4c** ($k_H = 4.8 \times 10^3$ M⁻¹ s⁻¹). The picture is, however, best envisaged when comparing compounds of the same O–H BDE and similarly hindered phenolic O–H moieties; thus **5d** outperforms **4b** by more than one order of magnitude ($k_{H(5d)}/k_{H(4b)} \sim 16$). Evidently we are facing an unusual rate enhancement as a consequence of the insertion of the two nitrogens in the phenolic ring. This phenomenon is maximum with alkyl radicals and moderate with peroxy radicals, while it is not observed with alkoxy radicals. The rate-enhancing effect also appears to become less and less important on increasing the electronic density at the aromatic ring; thus the electron-rich **5e** (BDE = 78.16 kcal mol⁻¹) is “only” five times more reactive than α -tocopherol (BDE = 78.23 kcal mol⁻¹) towards alkyl radicals, while the value of k_H for the electron-poor unsubstituted derivative **5a** (BDE = 90.3 kcal mol⁻¹) is two orders of magnitude higher than the corresponding k_H for phenol **4a** (BDE = 88.3 kcal mol⁻¹).

The possibility that the higher than expected reactivity of 5-pyrimidinols is due to some mechanism different from hydrogen-atom abstraction (e.g., by electron transfer from the antioxidant to the peroxy radical followed by fast proton exchange) can be clearly ruled out for several reasons. First, we have shown that both the calculated gas-phase adiabatic ionization potentials as well as the experimentally determined solution-phase oxidation potentials are higher in 5-pyrimidinols than in the equivalently-substituted phenols. Second, our EPR experiments revealed that the aryloxy radical is the only paramagnetic species generated in reactions of 5-pyrimidinols with alkoxy radicals. Furthermore, in our preliminary investigation,^[9] we studied the deuterium kinetic isotope effect (DKIE) on the reaction of 2,4,6-trimethyl-5-pyrimidinol with alkyl radicals and on that of 2-*N,N*-dimethylamino-4,6-dimethyl-5-pyrimidinol with peroxy radicals. The DKIE was measured as $k_H/k_D = 3.1$ for both reactions at 298 K. This value is in line with that previously observed with other antioxidants, such as phenols^[4] and aromatic amines,^[15] and is consistent with a primary DKIE; thus hydrogen abstraction

appears to be the mechanism for the radical scavenging by 5-pyrimidinols.

In our preliminary communication we suggested, as a possible explanation for the observed rate enhancement, the presence of polar effects,^[38] that is, that the transition state (TS) for hydrogen abstraction from 5-pyrimidinols might be stabilized by the contribution of ionic configurations to its wavefunction, therefore, reducing the activation energy required for hydrogen-atom transfer (as represented by the charge-separated resonance forms in Figure 7). We had

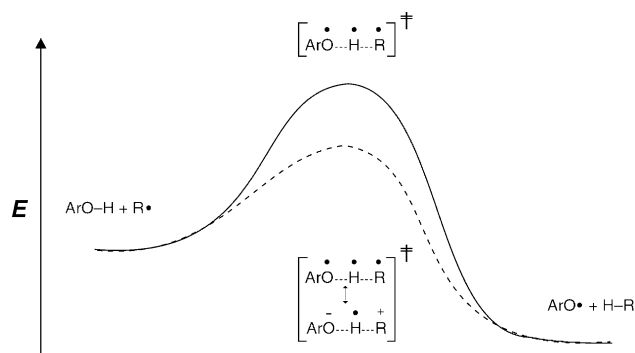


Figure 7. Reaction scheme for the hydrogen abstraction from phenols (Ar = Phenyl or C_6H_5 , solid line) and 5-pyrimidinols (Ar = Pyrimidyl or $C_4H_3N_2$, dotted line) by a radical species R^\bullet , illustrating the contribution of polar forms in the stabilization of the transition state.

suggested this explanation based upon the idea that the 5-pyrimidinol ring would accommodate a partial negative charge much better than the phenolic ring. This is supported by the experimental pK_a s for 5-pyrimidinol (6.8) and phenol (9.9).^[39] If such a mechanism is operating, this effect is expected to be more significant on the transition state involving the nucleophilic alkyl radicals compared to the electrophilic but polarizable peroxy radicals. Little or no stabilization of the TS is expected to come from forms in which a partial positive charge is placed on the electronegative "RO" moiety in hydrogen-atom abstractions by alkoxy radicals. These expectations are actually satisfied by the experimental observations with alkyl and peroxy radicals. The close to diffusion rate of hydrogen atom abstraction by alkoxy radicals does not allow us to appreciate a very minor contribution, if any, from polar effects. Furthermore, as it is actually observed, the contribution from polar forms is expected to decrease on increasing the ED character of substituents in the 5-pyrimidinol ring.

The calculations for the barrier heights corresponding to abstraction of the phenolic hydrogen atom by a methyl radical from phenol and 5-pyrimidinol are also consistent with the foregoing. Thus, despite the fact that the reaction of a methyl radical with phenol is more exothermic than the corresponding reaction with 5-pyrimidinol by about $2.5 \text{ kcal mol}^{-1}$ (calculated difference in O–H BDE between 5-pyrimidinol and phenol), the latter has a lower barrier by approximately $0.5 \text{ kcal mol}^{-1}$. This is contrary to the Hammond postulate and is inconsistent with the picture formed from previous work, which has shown that $\log k_H$ for phenols and alkyl radicals correlates very nicely with the O–H BDE.^[3] This further

supports the idea of some additional stabilization of the TS by charge separation.

The results for the calculated barrier heights for the reactions of phenol and 5-pyrimidinol with hydroperoxyl radical are different in that they correspond to the relative exothermicity of the reaction. The reaction of phenol with hydroperoxyl is roughly $0.5\text{--}1 \text{ kcal mol}^{-1}$ endothermic and the barrier is $8\text{--}9 \text{ kcal mol}^{-1}$. The corresponding reaction with 5-pyrimidinol is about $3.5 \text{ kcal mol}^{-1}$ endothermic and the barrier is $11\text{--}12 \text{ kcal mol}^{-1}$. These results are in line with the Hammond postulate and suggest that no major contribution, if any, is to be expected from polar effects in these reactions.

In order to obtain some experimental evidence that points more directly to a polar effect in the 5-pyrimidinol/alkyl radical reaction, we investigated the temperature dependence of the rate of hydrogen abstraction by alkyl radicals from 5-pyrimidinol **5d** (O–H BDE = $82.5 \text{ kcal mol}^{-1}$) and compared the measured activation energy (E_a) with the value available from similar studies^[3] for the essentially isothermal reaction of alkyl radicals with 2,4,6-trimethylphenol (**4b**, O–H BDE = $82.7 \text{ kcal mol}^{-1}$). The activation energy for the hydrogen abstraction from **4b** by 5-hexenyl radical in benzene had been previously reported by some of us as $E_a = 3.34 \text{ kcal mol}^{-1}$,^[3] while the corresponding term for **5d** and the neophyl radical was measured in this work to be $E_a = 0.64 \text{ kcal mol}^{-1}$. Despite the fact that these values are expected to have appreciable uncertainties due to the limited temperature range that we were able to investigate (ca. 60°C), the activation energy measured for the 5-pyrimidinol reaction is significantly lower than the value recorded for the phenol. Since the two compounds have essentially identical O–H BDEs, similar activation energies are expected for their reaction with alkyl radicals if no other factors affect the energy of the transition state.^[40] The E_a difference between the two reactions can therefore be taken as an estimate of the average contribution of the polar effect. Interestingly this value ($E_{a(5d)} - E_{a(4b)} = -2.7 \text{ kcal mol}^{-1}$) slightly overwhelms the unfavorable $\Delta\text{BDE}_{\text{OH}} \cong +2.5 \text{ kcal mol}^{-1}$ difference between 5-pyrimidinols and phenols, in good agreement with the theoretical data. We believe that these results taken together with the theoretical data and the preceding experimental data is compelling evidence that suggests the intervention of a polar effect in the atom transfer between 5-pyrimidinols and alkyl radicals. Unfortunately, whether or not a similar, but much attenuated, effect operates in reactions of 5-pyrimidinols and peroxy radicals remains unclear.

In their only appearances in the literature, 5-pyrimidinols have been described as having promising pharmacological activity. Indeed, compounds belonging to this class have been identified as potential anti-inflammatory and cyto-protective drugs, whose targets include lipooxygenases and cyclooxygenases.^[41] Since the actual mechanism of activity of 5-pyrimidinols has not been elucidated and since several radical species are known to be involved in the inflammatory processes,^[42] a fascinating hypothesis is that the radical scavenging ability of these compounds might actually play a role in their pharmacological activity. We are currently investigating this further.

Experimental Section

General procedures: Melting points were recorded on a Reichert Thermovar apparatus and are uncorrected. GC-MS was performed on a Hewlett–Packard 5890 Series II gas chromatograph coupled to a HP5971 Mass Selective Detector which was operated at EI⁺, 70 eV. High-resolution mass spectra were obtained on a VG 7070E double-analyzer spectrometer (EI⁺, 70 eV). NMR spectra were obtained by using a Varian Gemini 300 MHz with [D₆]DMSO as solvent except where noted. EPR spectra were recorded on a Bruker ESP 300 spectrometer equipped with a ER 033M FF-Lock and a temperature-control standard accessory, a Hewlett–Packard 5350B microwave frequency counter, and a NMR gaussmeter for the determination of the *g* factors, which were corrected with respect to that of the perylene radical cation in concentrated H₂SO₄ (*g* = 2.0025₈). Cyclic voltammetry was performed in acetonitrile with an EG&G PAR 273A potentiostat-galvanostat. UV-visible spectra were recorded in acetonitrile with a resolution of 1 nm using a Jasco V-550 spectrophotometer.

Materials: Solvents were of the highest grade available and were used without further purification. All compounds, except where otherwise noted, were commercially available (Aldrich, Fluka or Sigma) and were used as received. 2*R*,4*R*,8*R*-(*D*)-*α*-Tocopherol (Aldrich) was purified by column chromatography on silica gel according to a previously described method.^[26] Neophyl bromide (2-methyl-2-phenyl-1-bromopropane) was prepared from neophyl chloride (Aldrich) according to a literature procedure.^[43] 2-Methyl-2-(2-naphthyl)-1-bromopropane was prepared as previously described.^[21] Di-*tert*-butylperoxide (98%, Aldrich) was percolated through activated basic alumina and stored at 5 °C prior to use.

Synthesis of 5-methoxypyrimidine:^[44] 5-Bromopyrimidine (15 g, 90 mmol; Fluka) was treated with 5.4 g (0.1 mol) of sodium methoxide (Fluka) dissolved in methanol (170 mL) at 110 °C in a Parr reactor for 16 hours. The mixture was cautiously treated with water, neutralized with acetic acid, and extracted with diethyl ether (3 × 100 mL). After drying over Na₂SO₄, the solvent was removed under vacuum and the brown solid purified by column chromatography on silica gel (ethyl acetate/petroleum benzene 9:1) to yield 7 g (70%) of pale yellow crystals. M.p. 47–48 °C (lit. 47 °C^[44]); GC-MS: *m/z* (%): 110 (100) [M]⁺, 83 (14), 68 (98); ¹H NMR: δ = 3.88 (s, 3H), 8.53 (s, 2H), 8.78 (s, 1H).

Synthesis of 5-pyrimidinol (5a): Sodium hydride (3.38 g, 140.9 mmol; Aldrich, 60% suspension in mineral oil) was dissolved in dry DMF (60 mL) in fire-dried glassware to which ethanethiol (4.38 g, 70.4 mmol) was added dropwise. After stirring for 15 minutes, 5-methypyrimidine was added and the mixture is heated at 100 °C for 4 hours under argon. The brown suspension was then ice-cooled, water was added (100 mL), and the mixture neutralized with acetic acid and extracted in ethyl acetate (4 × 100 mL). The organic extract was dried over Na₂SO₄, the solvent evaporated under vacuum, and the yellow solid purified by column chromatography on silica gel eluting with ethyl acetate and crystallized from dioxane to yield **5a** (1.7 g, 50%) as white needles. M.p. 209–212 °C (lit. 209–211 °C^[10]); GC-MS: *m/z* (%): 96 (100) [M]⁺, 69 (5), 67 (1); ¹H NMR: δ = 8.33 (s, 2H), 8.66 (s, 1H), 10.45 ppm (s, 1H, exchanges with D₂O).

Synthesis of 2,4-dimethyl-5-acetyloxazole:^[11] 3-Chloropentan-2,4-dione (8 g, 59.4 mmol; Aldrich) and ammonium acetate (13.7 g, 178.2 mmol, 3 equiv) of were reacted in refluxing acetic acid (70 mL) for 4 hours. The mixture was then adjusted to pH 5 and extracted with diethyl ether (3 × 70 mL). The dried (Na₂SO₄) organic extract was evaporated under vacuum and the residue purified by column chromatography on silica gel (petroleum benzene/ethyl acetate 8:2) to yield the title compound as orange crystals (30%). M.p. 61 °C (lit. 61 °C^[11]); GC-MS: *m/z* (%): 139 (35) [M]⁺, 124 (11), 96 (40), 68 (100).

Synthesis of 2,4,6-trimethyl-5-pyrimidinol (5b):^[11] 2,4-Dimethyl-5-acetyloxazole (2.2 g, 15.8 mmol) was reacted with conc. aqueous ammonia (20 mL, 51 mmol) at 180 °C inside a Parr reactor for 10 hours. After cooling and adjusting to pH 5 by addition of conc. HCl, the organic material was extracted in diethyl ether (3 × 25 mL) and the extract dried over Na₂SO₄ and evaporated under vacuum. The solid was crystallized twice from benzene to yield compound **5b** as pale yellow crystals (60%). M.p. 153 °C (lit. 152–154 °C^[11]); GC-MS: *m/z* (%): 138 (100) [M]⁺, 123 (20), 109 (18), 95 (9), 82 (14), 69 (32); ¹H NMR: δ = 2.27 (s, 6H), 2.36 (s, 3H), 8.86 ppm (s, 1H, exchanges with D₂O).

Synthesis of 4-bromo-2,2,6,6-tetramethylheptan-3,5-dione:^[45] Bromine (16.4 g, 0.1 mol) was added dropwise to a stirred solution of 2,2,6,6-tetramethylheptan-3,5-dione (25 g, 0.13 mol; Aldrich) dissolved in CCl₄ (150 mL). After stirring for 30 min at room temperature the solvent was removed under reduced pressure and the resulting yellow oil diluted with diethyl ether (200 mL), and washed with water (200 mL), NaHCO₃ 0.5 M (200 mL), and sodium thiosulphate 0.5 M (200 mL). After drying (Na₂SO₄), the solvent was removed and residue crystallized from hexane at –18 °C to yield 24.7 g (73%) of title product as white crystals. M.p. 45 °C (lit. 44–45 °C^[45]); GC-MS: *m/z* (%): 262–264 (0.1) [M]⁺, 178–180 (15), 163–165 (2), 127 (43), 57 (100); ¹H NMR (CDCl₃): δ = 1.26 (s, 18H), 5.66 ppm (s, 1H).

Synthesis of 2-methyl-4-*tert*-butyl-5-(2,2-dimethylpropanoyl)oxazole:^[12] 4-Bromo-2,2,6,6-tetramethylheptan-3,5-dione (1.5 g, 5.7 mmol) and ammonium acetate (2.63 g, 34.2 mmol) were refluxed in acetic acid (60 mL) for 27 hours. The mixture was diluted with water adjusted to pH 5 by adding NaOH 0.5 M and extracted with ethyl acetate (3 × 20 mL). The dried (Na₂SO₄) organic solution was concentrated under reduced pressure to yield an orange oil that is purified by column chromatography on silica gel (petroleum ether/ethyl acetate 8:2). Yield: 1.25 g (98%); GC-MS: *m/z* (%): 223 (1) [M]⁺, 208 (1), 166 (31), 138 (65), 82 (32), 69 (73), 57 (100); ¹H NMR (CDCl₃): δ = 1.29 (s, 9H), 1.35 (s, 9H), 2.09 ppm (s, 3H).

Synthesis of 2-methyl-4,6-di-*tert*-butyl-5-pyrimidinol (5c):^[12] 2-Methyl-4-*tert*-butyl-5-(2,2-dimethylpropanoyl)oxazole (1.25 g, 5.6 mmol) was heated at 180 °C for 36 hours in a Parr bomb in the presence conc. aqueous ammonia (100 mL). After removal of the excess ammonia under reduced pressure, the pH of the solution was adjusted to pH 6 by addition of conc. HCl. The organic material was then extracted in diethyl ether, which was subsequently removed under vacuum after drying over Na₂SO₄. Purification by column chromatography on silica gel (petroleum ether/ethyl acetate 8:2) yields 0.87 g (70%) of compound **5c** as white crystals. M.p. 55–56 °C; GC-MS: *m/z* (%): 222 (14) [M]⁺, 207 (100), 180 (86), 165 (24), 138 (21), 69 (24); HRMS: *m/z*: calcd for C₁₃H₂₂N₂O 222.1732; found: 222.1734; ¹H NMR: δ = 1.33 (s, 18H), 2.41 (s, 3H), 7.74 ppm (s, 1H, exchange with D₂O); ¹³C NMR: δ = 25.36, 28.86, 37.33, 144.98, 156.51, 165.35 ppm.

Synthesis of 3-benzyloxypentan-2,4-dione: Sodium benzoate (35.5 g, 0.25 mol) and 3-chloropentan-2,4-dione (16.7 g, 0.12 mol) were reacted in anhydrous DMSO as described for 4-benzyloxy-2,2,6,6-tetramethylheptan-3,5-dione. The addition of water followed by extraction in diethyl ether afforded the title compound as a light orange oil (27.1 g; 100%). GC-MS: *m/z* (%): 220 (0.1) [M]⁺, 178 (10), 105 (100), 77 (40); ¹H NMR (CDCl₃): δ = 2.39 (s, 6H), 5.72 (s, 1H), 7.50 (m, 2H), 7.64 (t, *J* = 8 Hz, 1H), 8.12 ppm (d, *J* = 7 Hz, 2H).

Synthesis of 2-methoxy-4,6-dimethyl-5-benzyloxypyrimidine: 3-Benzyloxypentan-2,4-dione (3.2 g, 14.9 mmol) was added to of *O*-methylisourea hydrogen sulphate (2.56 g, 14.9 mmol; Aldrich) and sodium acetate (2.4 g, 29.8 mmol) in anhydrous DMF (50 mL) under argon. The suspension was stirred overnight at 100 °C, then cooled, diluted with water (50 mL), neutralized with acetic acid, and extracted with diethyl ether (3 × 25 mL); the organic layers were then dried (Na₂SO₄) and the solvent removed under vacuum. The residue was purified by column chromatography on silica gel (petroleum ether/ethyl acetate 8:2) to yield 0.7 g (20%) of the title compound. GC-MS: *m/z* (%): 258 (5) [M]⁺, 227 (0.1), 125 (1), 105 (100), 77 (32); ¹H NMR: δ = 2.24 (s, 6H), 3.88 (s, 3H), 7.47 (m, 2H), 7.69 (t, *J* = 8 Hz, 1H), 8.17 ppm (d, *J* = 7 Hz, 2H).

Synthesis of 2-methoxy-4,6-dimethyl-5-pyrimidinol (5d): The protected 5-pyrimidinol (0.7 g, 2.7 mmol) was treated with KOH (0.3 g, 5.4 mmol) in refluxing ethanol for 10 hours. After cooling and diluting with water, the solution was adjusted to pH 5 by addition of acetic acid and extracted in ethyl acetate. After drying (Na₂SO₄), the solvent was removed under vacuum and the residue purified by column chromatography on silica gel (petroleum ether/ethyl acetate 9:1) to yield 0.4 g (98%) of white crystals. M.p. 89–90 °C; GC-MS: *m/z* (%): 154 (100) [M]⁺, 124 (73), 95 (16) 82 (18); HRMS: *m/z* (%): calcd for C₇H₁₀N₂O₂: 154.0742; found: 154.0741; ¹H NMR: δ = 2.27 (s, 6H), 3.75 (s, 3H), 8.56 ppm (s, 1H, exchanges with D₂O); ¹³C NMR (CD₃OD): δ = 18.83, 55.02, 144.19, 158.02, 210.02 ppm.

Synthesis of 3-acetoxypentan-2,4-dione: 3-Chloropentan-2,4-dione (10 g, 74.6 mmol; Aldrich) was treated with sodium acetate (12.2 g, 149.2 mmol) in anhydrous DMSO for 3 hours at room temperature. After addition of water, the product was extracted in diethyl ether, and the organic solution

dried (Na_2SO_4) and concentrated under vacuum. The residue was purified by column chromatography on silica gel (petroleum ether/ethyl acetate 8:2) to yield 9.2 g (80%) of the title compound. GC-MS: m/z (%): 158 (10) [M]⁺, 116 (87), 101 (28), 74 (100); ¹H NMR (CDCl_3): δ = 2.02 (s, 3H), 2.23 (s, 6H), 5.48 (s, 1H).

Synthesis of 2-dimethylamino-4,6-dimethyl-5-pyrimidinol (5e):^[13] 3-Acetoxy-pentan-2,4-dione (1.0 g, 6.3 mmol), sodium acetate (1.0 g, 12.6 mmol), and 1,1-dimethylguanidine sulphate (1.7 g, 6.3 mmol; Aldrich) were suspended in anhydrous DMF (70 mL) under argon and the mixture was stirred for 4 hours at 100 °C. After dilution with water, the resulting solution was extracted with ethyl acetate (3 × 25 mL), the dried (Na_2SO_4) extract concentrated under reduced pressure, and the resulting orange oil subjected to column chromatography on silica gel (petroleum ether/ethyl acetate 8:2). The title product was crystallized from benzene/petroleum ether to yield 0.39 g of pale yellow needles (30%). M.p. 149–151 °C; GC-MS: m/z (%): 167 (85) [M]⁺, 152 (100), 138 (87), 124 (38), 69 (20); HRMS: m/z (%): calcd for $\text{C}_8\text{H}_{13}\text{N}_3\text{O}$: 167.1059; found: 167.1057; ¹H NMR: δ = 2.18 (s, 6H), 2.97 (s, 6H), 7.84 ppm (brs, 1H, exchanges with D_2O); ¹³C NMR (CDCl_3): δ = 20.50, 37.52, 134.08, 154.69, 157.33 ppm.

Synthesis of 4-benzyloxy-2,2,6,6-tetramethylheptan-3,5-dione: Sodium benzoate (20.3 g, 0.14 mol; Aldrich) and 4-bromo-2,2,6,6-tetramethylheptan-3,5-dione (24.7 g, 0.094 mol) were mechanically stirred in anhydrous DMSO (250 mL) for 3 hours under argon. After cooling (0 °C) and diluting with water the title compound crystallized as a pure white solid. Yield 28.0 g (99%); M.p. 82 °C (lit. 85 °C^[46]); GC-MS: m/z (%): 304 (0.1) [M]⁺, 298 (0.1), 247 (0.1), 220 (5), 105 (100), 86 (5), 77 (20); ¹H NMR (CDCl_3): δ = 1.25 (s, 18H), 6.46 (s, 1H), 7.47 (m, 2H), 7.61 (t, J = 8 Hz, 1H), 8.08 ppm (d, J = 9 Hz, 2H).

Synthesis of 2-dimethylamino-4,6-di-*tert*-butyl-5-pyrimidinol (5f): 4-Benzyloxy-2,2,6,6-tetramethylheptan-3,5-dione (1.0 g, 3.29 mmol) was added to a stirred suspension of 1,1-dimethylguanidine sulphate (0.87 g, 3.29 mmol) and K_2CO_3 (0.9 g, 6.5 mmol) in anhydrous DMF (30 mL) under argon. The suspension was vigorously stirred overnight at 65 °C then diluted with water (50 mL) and extracted with diethyl ether, which was then removed under reduced pressure after drying over Na_2SO_4 . The dark oil was purified by column chromatography on silica gel (petroleum ether/dichloromethane 9:1) to yield compound 5f as colorless crystals (80 mg; 10%). M.p. 65–66 °C; GC-MS: m/z (%): 251 (90) [M]⁺, 236 (92), 222 (31), 209 (96), 194 (28), 167 (43); HRMS: m/z (%): calcd for $\text{C}_{14}\text{H}_{25}\text{N}_3\text{O}$: 251.1998; found: 251.1998; ¹H NMR: δ = 1.32 (s, 18H), 3.02 (s, 6H), 6.90 ppm (s, 1H, exchanges with D_2O); ¹³C NMR (CDCl_3): δ = 28.70, 37.13, 37.55, 138.64, 156.08, 163.29 ppm.

Measurement of O–H BDEs: A deoxygenated benzene solution containing the 5-pyrimidinol under investigation (0.01–1M), an appropriate reference phenol (0.1–0.2M) and di-*tert*-butyl peroxide (0.1M) was sealed under nitrogen in a suprasil quartz EPR tube sitting inside the thermostatted cavity of an EPR spectrometer. Photolysis was carried out by focusing the unfiltered light from a 500 W high-pressure mercury lamp on the EPR cavity. With compounds originating relatively persistent radical species (i.e., aryloxy radicals showing no decay during an EPR field-sweep) a short (1–5 s) UV pulse was used, while with the less persistent radicals continuous photolysis was necessary to establish “radical buffer” conditions.^[2] The temperature was controlled with a standard variable temperature accessory and was monitored before and after each run with a copper-constantan thermocouple. Relative radical concentrations were determined by comparing the double integrals of at least two lines of the equilibrating species or, when strong line overlap was present, by comparison of the digitized experimental spectra with computer simulated ones. In these cases an iterative least-squares fitting procedure based on the systematic application of the Monte–Carlo method was performed in order to obtain the experimental spectral parameters of the two species including their relative intensities.

Kinetic measurements

Reactivity toward alkyl radicals: In a typical experiment, 200 μL of a solution of the 5-pyrimidinol under investigation (0.001–0.1M) containing either neophyl bromide, 2-methyl-2-(2-naphthyl)-1-propyl bromide or 6-bromo-1-hexene (0.005–0.01M) and bis(tributyltin) (0.001–0.001M) were sealed in a quartz tube, after being deoxygenated by bubbling nitrogen. The initial concentration of 5-pyrimidinol was chosen to be high enough to avoid significant consumption during irradiation, yet low enough to avoid

self-association.^[3] The reaction mixture was then irradiated for 15–30 minutes at the desired temperature in a suitable thermostatted photoreactor built in our laboratories, equipped with a 125 W high-pressure mercury lamp, and analyzed by gas chromatography by means of direct injection and a wide-bore HP-5 column (30 m, 0.53 mm × 2.65 μm film thickness). The identity of the hydrocarbons to be detected was checked in a preliminary set of experiments by using GC-MS and authentic samples as standard reference. For each 5-pyrimidinol, in each solvent, 4–7 measurements were made at the desired temperature with different substrate concentration and the reaction products’ ratio $[\text{RH}]/[\text{R}^{\cdot}\text{H}]$ was plotted versus the 5-pyrimidinol concentration in order to obtain the $k_{\text{H}}/k_{\text{r}}$ ratio by linear regression of the experimental data.

Reactivity toward alkoxy radicals: A solution of di-*tert*-butyl peroxide (0.01–0.1M), a 5-pyrimidinol (ca. 10 – 500×10^{-3} M), tris(trimethylsilyl)silane (1 – 500×10^{-3} M) as reference hydrogen donor and *tert*-butylbenzene as internal GC standard, in benzene, was degassed and sealed under nitrogen in quartz ampules. For some of the compounds measurements were repeated using tributyltin hydride (10 – 100×10^{-3} M) as competing hydrogen donor. For the less reactive compounds 5a,b triphenylsilane was used in place of TTMSS. The reaction mixture was photolyzed at 298 K for 15–30 minutes in a thermostatted photoreactor equipped with a 125 W high-pressure mercury lamp, and the disappearance of the products was analyzed by GC. For each compound, the results were averaged over 3–5 measurements with different 5-pyrimidinol/silane concentrations.

Reactivity toward peroxy radicals: The autoxidation experiments were performed on solutions of styrene (5.2M) in benzene containing the desired 5-pyrimidinol (5×10^{-6} – 1×10^{-3} M), AIBN (1×10^{-3} – 4×10^{-2} M) as thermal initiator, and the stable nitroxide TEMPO (ca. 5×10^{-6} M) that were air saturated at room temperature and introduced (ca. 200 μL) into a capillary tube with the internal diameter of about 1.85 mm. A second capillary tube (external diameter of 1.60 mm) sealed at one end was introduced into the sample tube so to leave very little dead volume space. The tube was sealed and put into the EPR cavity kept at 50 °C and the first spectrum was recorded after approximately 1 minute to allow for temperature equilibration time.

Initiation rates: $R_i = 2[\alpha\text{-tocopherol}]/\tau$, whereby τ is the length of the inhibition period under experimental conditions such that the chain length is 1, that is, any peroxy radical deriving from the decomposition of the initiator (and subsequent reaction with molecular oxygen) reacts with α -tocopherol. In all the other experiments (i.e., when k_{inh} was to be measured) care was taken to ensure that the chain length was 8 or higher during the inhibited period.

The EPR spectra were recorded at regular intervals on a Bruker ESP 300 spectrometer by using the following settings: microwave frequency 9.74 GHz, power 6.4 mW, modulation amplitude 0.7 G, center field 3320 G, sweep time 81 s and time constant 81 ms. For each spectra the amount of oxygen still present in the sample was determined from the intensity (I) of the first spectral line of TEMPO, after calibration of the spectrometer response, according to a previously described method: $I^{-1/2} \propto W_{\text{int}} + 4\pi r D_{\text{ox}}[\text{O}_2]^{[32]}$ whereby W_{int} is the intrinsic line width of TEMPO, and D_{ox} is the diffusion coefficient of oxygen in the solvent employed.

Electrochemical measurements: Electrochemical experiments on platinum (PtE) and glassy carbon electrodes (GCE) were performed by cyclic voltammetry (CV) by using a three-electrode cell with separated compartments in an Ar-filled Mbraun Labmaster 130 dry-box (oxygen and water content < 1 ppm) at room temperature. A reference electrode Ag/AgNO₃ 1.0×10^{-2} M in CH_3CN was used, and all the potential data in the text are corrected to be versus saturated calomel electrode (SCE). The CVs were performed in CH_3CN that contained 0.5 M Et_4NBF_4 with electroactive molecule concentration ≤ 2.5 mM, related to the molecule solubility, with scan rate in the range 50–200 mV s^{-1} . The CH_3CN (Fluka) was a reagent grade product carefully distilled and dried over molecular sieves before use, and Et_4NBF_4 (Fluka) was electrochemical grade product dried at 80 °C under dynamic vacuum overnight. The water content in the solvent and in the solutions, 30 ppm and 45 ppm respectively, were checked with a Metrohm 684 KF coulometer.

Method of calculation: The methods for calculating O–H bond dissociation enthalpies and ionization potentials of all compounds have been described elsewhere.^[47, 48] For the species involved in barrier height calculations, geometry optimizations were performed using the B3LYP functional^[49]

with a 6–31+G(d,p) basis set. For hydrogen-atom abstractions by hydroperoxyl, the hydrogen-bonded pre- and post-reaction complex structures were also determined. Minima were verified by performing vibrational frequency calculations. Vibrational frequencies were scaled by 0.9806 as suggested by Scott and Radom.^[50] In general, the transition state structures were found using the STQN algorithm of Ayala and Schlegel,^[51] with the OPT=QST2 or OPT=QST3 keywords in Gaussian-98.^[52] In some cases, a guess at the transition-state structure was obtained from a failed QST2 calculation and used in a subsequent QST3 calculation. This procedure was usually successful. Transition-state structures were verified by the presence of a single negative vibrational mode corresponding to the reaction path connecting reactants and products. Additional single-point energy calculations were performed on all structures at the B3LYP/6–311+G(2d,2p) and MPW1K/6–31+G(d,p)^[54] levels for comparison.

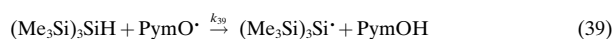
Acknowledgements.

We thank Prof. Domenico Spinelli for helpful discussion and Dr. Luca Zuppiroli for assistance with HRMS. This project was in part supported by the University of Bologna and the MIUR Research project “Free Radical Research in Chemistry and Biology: Fundamental Aspects and Applications in Environment and Material Science”. DAP thanks NSERC Canada, Vanderbilt University and Professor Ned A. Porter for their support.

- [1] a) L. J. Marnett, *Carcinogenesis* **2000**, *21*, 361–370; b) A. Sevanian, F. Ursini, *Free Radical Biol. Med.* **2000**, *29*, 306–311; c) D. Steinburg, S. Parhsarathy, T. E. Carew, J. C. Khoo, J. L. Witztum, *N. Engl. J. Med.* **1989**, *320*, 915–924; d) G. M. Chisholm, D. Steinburg, *Free Radical Biol. Med.* **2000**, *28*, 1815–1826.
- [2] a) M. Lucarini, P. Pedrielli, G. F. Pedulli, S. Cabiddu, C. Fattuoni, *J. Org. Chem.* **1996**, *61*, 9259–9263; b) M. Lucarini, G. F. Pedulli, M. Cipollone, *J. Org. Chem.* **1994**, *59*, 5063–5070 and references therein.
- [3] P. Franchi, M. Lucarini, G. F. Pedulli, L. Valgimigli, B. Lunelli, *J. Am. Chem. Soc.* **1999**, *121*, 507–514.
- [4] a) G. W. Burton, T. Doba, E. J. Gabe, L. Hughes, F. L. Lee, L. Prasad, K. U. Ingold, *J. Am. Chem. Soc.* **1985**, *107*, 7053–7065; b) G. W. Burton, K. U. Ingold, *Acc. Chem. Res.* **1986**, *19*, 194–201.
- [5] J. S. Wright, E. R. Johnson, G. A. DiLabio, *J. Am. Chem. Soc.* **2001**, *123*, 1173–1183.
- [6] See for example: J. Alanko, A. Riutta, P. Holm, I. Mucha, H. Vapaatalo, T. Metsa-Ketela, *Free. Radical Biol. Med.* **1999**, *26*, 193–201; M. Manno, C. Ioannides, G. G. Gibson, *Toxicol. Lett.* **1985**, *25*, 121–130.
- [7] J. S. Wright, D. A. Pratt, G. A. DiLabio, T. P. Bender, K. U. Ingold, *Cancer Detect. Prev.* **1998**, *22*, 204.
- [8] M. C. Foti, E. R. Johnson, M. R. Vinqvist, J. S. Wright, L. R. C. Barclay, K. U. Ingold, *J. Org. Chem.* **2002**, *67*, 5190–5196.
- [9] D. A. Pratt, G. A. DiLabio, G. Brigati, G. F. Pedulli, L. Valgimigli, *J. Am. Chem. Soc.* **2001**, *123*, 4625–4626.
- [10] H. Bredereck, F. Effenberger, H. E. Schweizer, *Chem. Ber.* **1962**, *95*, 803–809.
- [11] A. Dornow, H. Hell, *Chem. Ber.* **1960**, *93*, 1998–2001.
- [12] P. C. Unangst, D. T. Connor, C. R. Kostlan, G. P. Shrum, S. R. Miller, G. Kanter, *J. Heterocycl. Chem.* **1995**, *32*, 1197–1200; D. T. Connor, C. R. Kostlan, US Pat. 5,177,079, January 5, **1993**.
- [13] F. J. Walker, J. L. LaMattina, US Pat. 4,711,888 December 8, **1987**.
- [14] F. J. Walker, K. G. Kraus, *J. Heterocycl. Chem.* **1987**, *24*, 1485–1486; J. L. LaMattina, C. J. Mularski, *Tetrahedron Lett.* **1984**, *25*, 2957–2960.
- [15] M. Lucarini, P. Pedrielli, G. F. Pedulli, L. Valgimigli, D. Gigmes, P. Tordo, *J. Am. Chem. Soc.* **1999**, *121*, 11546–11553.
- [16] D. Griller, K. U. Ingold, *Acc. Chem. Res.* **1980**, *13*, 317–323.
- [17] M. Newcomb, *Tetrahedron* **1993**, *49*, 1151–1176.
- [18] C. Chatgililoglu, K. U. Ingold, J. C. Scaiano, *J. Am. Chem. Soc.* **1981**, *103*, 7739–7742.
- [19] a) J. A. Franz, R. D. Barrows, D. M. Camaioni, *J. Am. Chem. Soc.* **1984**, *106*, 3964–3967; b) A. Burton, K. U. Ingold, J. C. Walton, *J. Org. Chem.* **1996**, *61*, 3778–3782.
- [20] This value was preferred to the newer value of $4 \times 10^2 \text{ s}^{-1}$ obtained by Fischer and co-workers (M. Weber, H. Fisher, *J. Am. Chem. Soc.* **1999**,

121, 7381–7388), because when the same compound was calibrated with two different clocks, the older value provided a generally better agreement between the neophyl-based measurement and that obtained with 5-hexenyl or 2-methyl-2-(2-naphtyl)-1-propyl radical.

- [21] R. Leardini, M. Lucarini, G. F. Pedulli, L. Valgimigli, *J. Org. Chem.* **1999**, *64*, 3726–3730.
- [22] When the neophyl or 2-methyl-2-(2-naphtyl)-1-propyl radicals were used as radical clocks, very small amounts of side products were observed. Thus, in addition to the expected *tert*-butylbenzene and *iso*-butylbenzene, or 2-*tert*-butylnaphtalene and 2-isobutylnaphtalene, that represent the unrearranged and rearranged hydrocarbons of the neophyl and MNP radicals, we also observed 1-phenyl-2-methylpropene or 1-(2-naphtyl)-2-methylpropene as identified on the basis of their mass spectra. These hydrocarbons are known to originate from the disproportionation of the rearranged radical R',^[19b] and as such, the denominator in Equation (18) has been adjusted accordingly.
- [23] M. J. Kamlet, J.-L. M. Abboud, M. H. Abraham, R. W. Taft, *J. Org. Chem.* **1983**, *48*, 2877–2887.
- [24] The β_s values used in the regression were 0.31, 0.45, and 0.55 for acetonitrile, ethyl acetate, and *tert*-butanol, respectively.
- [25] D. V. Avila, K. U. Ingold, J. Luszytky, W. H. Green, D. R. Procopio, *J. Am. Chem. Soc.* **1995**, *117*, 2929–2930.
- [26] L. Valgimigli, J. T. Banks, K. U. Ingold, J. Luszytky, *J. Am. Chem. Soc.* **1995**, *117*, 9966–9971.
- [27] C. Chatgililoglu, S. Rossini, *Bull. Soc. Chim. Fr.* **1988**, 298–300.
- [28] C. Chatgililoglu, K. U. Ingold, J. Luszytky, A. S. Narzan, J. C. Scaiano, *Organometallics*, **1983**, *2*, 1332–1335.
- [29] C. K. Ingold, F. R. Shaw, *J. Chem. Soc.* **1927**, 2918–2926.
- [30] In principle, the results obtained by competition kinetics of this kind might be affected by the hydrogen-atom exchange between the silane and the 5-pyrimidinoyl radical. If this reaction is fast enough it might regenerate some 5-pyrimidinol [Eq. (39)], thus resulting in an underestimation of rate constant k_{21} .



To check the relevance of the reaction in Equation (39), the time-dependence of the EPR signal of the photolytically generated 5-pyrimidinoyl radical (PymO*) for compounds **5c** and **5e** was followed both in the absence and in the presence of variable amounts of TTMSS. From these experiments it could be concluded that for both 5-pyrimidinols (and conceivably for any other reported in this work) the rate constant of reaction is $k_{39} < 1 \text{ M}^{-1} \text{ s}^{-1}$ and can therefore be neglected under our experimental conditions. One additional source of error in the competition kinetics relying on the measurement of the loss of starting material both for the compound under investigation and the reference compound arises from side reactions consuming one or both of the competing reactants. Since some of the measurements herein reported were performed with starting concentrations of pyrimidinol comparable to the concentration of radical initiator (di-*tert*-butylperoxide) and considering the relatively high absorbance of 5-pyrimidinols in the UV spectral region corresponding to the Hg-lamp emission (see Table 7) it is possible that direct photolysis of the pyrimidinol occurs to some extent which would be reflected in an overestimation of their rate of reaction with alkoxy radicals. We thank a referee for pointing this out. However it should be noted that: 1) when benzene solutions of pyrimidinols **5c–f** were irradiated directly in the cavity of an EPR spectrometer in the absence of any radical initiator, incident radiations 50–100 times more intense of those employed in the competition kinetics were necessary to observe EPR signals due to the corresponding aryloxy radicals (presumably originated by photoionization followed by fast proton transfer), while no signal could be observed for pyrimidinols **5a,b**; 2) kinetic measurement performed with different initial amounts of pyrimidinol (leading to a different extent of direct photolysis) afforded almost identical results; 3) kinetic measurements based on this competitive approach were performed under identical experimental conditions on α -tocopherol (for which direct photolysis is a known process and which has an ionization potential lower than all of the pyrimidinols) affording rate constants values very close to those, previously reported (ref. [26]), obtained by laser flash photolysis

- direct measurements. Direct photolysis of pyrimidinols was therefore judged to be of marginal importance under our experimental conditions.
- [31] J. A. Howard, in *Free Radicals Vol. 2* (Ed.: J. K. Kochi), Wiley, New York, **1973**, Chapter 12.
- [32] a) M. Cipollone, C. Di Palma, G. F. Pedulli, *Appl. Magn. Res.* **1992**, *3*, 99–106; b) G. F. Pedulli, M. Lucarini, P. Pedrielli, M. Sagrini, M. Cipollone, *Res. Chem. Intermed.* **1996**, *22*, 1–14; c) M. Lucarini, G. F. Pedulli, L. Valgimigli, *J. Org. Chem.* **1998**, *63*, 4497–4499.
- [33] V. M. Darley-Usmar, A. Hersey, L. G. Garland, *Biochem. Pharm.* **1989**, *38*, 1465–1469.
- [34] B. J. Lynch, P. L. Fast, M. Harris, D. G. Truhlar, *J. Phys. Chem. A* **2000**, *104*, 4811–4815.
- [35] B. J. Lynch, D. G. Truhlar, *J. Phys. Chem. A* **2001**, *105*, 2936–2941.
- [36] See for instance: K. Vessman, M. Ekström, M. Berglund, C.-M. Andersson, L. Engman, *J. Org. Chem.*, **1995**, *60*, 4461–4467; D. W. Brown, P. R. Graupner, M. Sainsbury, H. G. Shertz, *Tetrahedron*, **1991**, *47*, 4383–4408.
- [37] Steric hindrance around the –OH moiety is known to play a major role in decreasing the reactivity of phenolic compounds toward hydrogen abstraction. See references [1]–[3].
- [38] C. Walling, *Free Radicals in Solution*, Wiley, New York, **1957**; P. Khaushal, P. L. H. Mok, B. P. Roberts, *J. Chem. Soc. Perkin Trans. 2*, **1990**, 1663–1670; F. Minisci, A. Citterio, *Adv. Free Radical Chem.* **1980**, *6*, 65–153; “Substituent Effects in Radical Chemistry”: *NATO ASI Ser. C* **1986**, *189*, whole volume.
- [39] The pK_a s of 5-pyrimidinol and phenol are 6.8 and 9.9, respectively, in H_2O at 25 °C; see: S. F. Mason, *J. Chem. Soc.* **1958**, 674–685; A. E. Castro, P. Pavez, J. G. Santos, *J. Org. Chem.* **1999**, *64*, 2310–2313.
- [40] The use of different radical clocks to time the hydrogen abstraction from the two substrates (5-hexenyl radical for phenol **4b**^[3] and neophyl radical for pyrimidinol **5d**) is expected to give only a minor contribution (if any) to the observed difference in activation energy, since they give rise to the formation of C–H bonds or approximately equal BDE (about 98 kcal mol⁻¹ by Benson’s rule, see S. W. Benson, *Thermochemical Kinetics*, Wiley, New York, **1976**) and contributing approximately the same “triplet repulsion” term (see A. A. Zavitsas, C. Chatgililoglu, *J. Am. Chem. Soc.* **1995**, *117*, 10645–10654).
- [41] F. J. Walker, US Pat. 5,001,136 March 19, **1991**.
- [42] See for instance: J. A. Badway, M. L. Karnovsky, *Ann. Rev. Biochem.* **1980**, *49*, 695–726; B. Halliwell, *Am. J. Med.* **1991**, *91*, 145–225; M. Valgimigli, L. Valgimigli, D. Trere, S. Gaiani, G. F. Pedulli, L. Gramantieri, L. Bolondi, *Free. Radical. Res.* **2002**, *36*, 939–948.
- [43] A. H. Fainberg, S. Winstein, *J. Am. Chem. Soc.* **1956**, *78*, 2763–2767.
- [44] H. Bredereck, R. Gommpper, H. Herling, *Chem. Ber.* **1958**, *91*, 2832–2849.
- [45] C. W. Shoppee, D. Stevenson, *J. Chem. Soc. Perkin Trans. 1*, **1972**, 3015–3020.
- [46] D. Barillier, *Phosphorus Sulfur Relat. Elem* **1978**, *5*, 251–254.
- [47] G. A. DiLabio, D. A. Pratt, A. D. LoFaro, J. S. Wright, *J. Phys. Chem. A* **1999**, *103*, 1653–1661.
- [48] a) G. A. DiLabio, D. A. Pratt, J. S. Wright, *Chem. Phys. Lett.* **1999**, *311*, 215–220; b) G. A. DiLabio, D. A. Pratt, J. S. Wright, *J. Org. Chem.* **2000**, *65*, 2195–2203.
- [49] A. D. Becke, *J. Chem. Phys.* **1993**, *98*, 5648–5652; C. Lee, W. Yang, R. G. Parr, *Phys. Rev. B* **1988**, *37*, 785–789.
- [50] A. P. Scott, L. Radom, *J. Phys. Chem.* **1996**, *100*, 16502–16513.
- [51] P. Y. Alaya, H. B. Schlegel, *J. Chem. Phys.* **1997**, *107*, 375–384.
- [52] Gaussian 98 (Revision A.7), M. J. Frisch, G. W. Trucks, H. B. Schlegel, G. E. Scuseria, M. A. Robb, J. R. Cheeseman, V. G. Zakrzewski, J. A. Montgomery, R. E. Stratmann, J. C. Burant, S. Dapprich, J. M. Millam, A. D. Daniels, K. N. Kudin, M. C. Strain, O. Farkas, J. Tomasi, V. Barone, M. Cossi, R. Cammi, B. Mennucci, C. Pomelli, C. Adamo, S. Clifford, J. Ochterski, G. A. Petersson, P. Y. Ayala, Q. Cui, K. Morokuma, D. K. Malick, A. D. Rabuck, K. Raghavachari, J. B. Foresman, J. Cioslowski, J. V. Ortiz, B. B. Stefanov, G. Liu, A. Liashenko, P. Piskorz, I. Komaromi, R. Gomperts, R. L. Martin, D. J. Fox, T. Keith, M. A. Al-Laham, C. Y. Peng, A. Nanayakkara, C. Gonzalez, M. Challacombe, P. M. W. Gill, B. G. Johnson, W. Chen, M. W. Wong, J. L. Andres, M. Head-Gordon, E. S. Replogle, J. A. Pople, Gaussian, Inc., Pittsburgh, PA, **1998**.

Received: March 17, 2003 [F4960]